Molecular Level Understanding of Adhesion Mechanisms at the Epoxy/Polymer Interfaces

ARTICLE *in* ACS APPLIED MATERIALS & INTERFACES · JUNE 2012

Impact Factor: 6.72 · DOI: 10.1021/am300854g · Source: PubMed

3 AUTHORS, INCLUDING:

Chi Zhang
Purdue University
33 PUBLICATIONS **222** CITATIONS
SEE PROFILE

Jeanne M Hankett
University of Michigan
13 PUBLICATIONS **143** CITATIONS
SEE PROFILE

ACS APPLIED MATERIALS & INTERFACES

Research Article

www.acsami.org

Molecular Level Understanding of Adhesion Mechanisms at the Epoxy/Polymer Interfaces

Chi Zhang, Jeanne Hankett, and Zhan Chen*

Department of Chemistry, University of Michigan, Ann Arbor, Michigan 48109, United States

Supporting Information

ABSTRACT: It is important to understand the buried interfacial structures containing epoxy underfills as such structures determine the interfacial adhesion properties. Weak adhesion or delamination at such interfaces leads to failure of microelectronic devices. Sum frequency generation (SFG) vibrational spectroscopy was used to examine buried interfaces at polymer/model epoxy and polymer/commercial epoxy resins (used as underfills in flip chip devices) at the molecular level. We investigated a model epoxy: bisphenol A digylcidyl ether (BADGE) at the interfaces of poly (ethylene terephthalate) (PET) before and after curing. Furthermore, small amounts of different silanes including (3-glycidoxypropyl) trimethoxysilane (γ-GPS), (3-Aminopropyl)trimethoxysilane (ATMS), Octadecyltrimethoxysilane (OTMS(18C)), and Octyltrimethoxysilane (OTMS(8C)) were mixed with BADGE. Silane influences on the polymer/epoxy interfacial structures were studied. SFG was also used to study molecular interfacial structures between polymers and two commercial epoxy resins. The interfacial structures probed by SFG were correlated to the adhesion strengths measured for corresponding interfaces. The results indicated that a small amount of silane molecules added to epoxy could substantially change the polymer/epoxy interfacial structure, greatly affecting the adhesion strength at the interface. It was found that ordered methyl groups at the interface lead to weak adhesion, and disordered interfaces lead to strong adhesion.

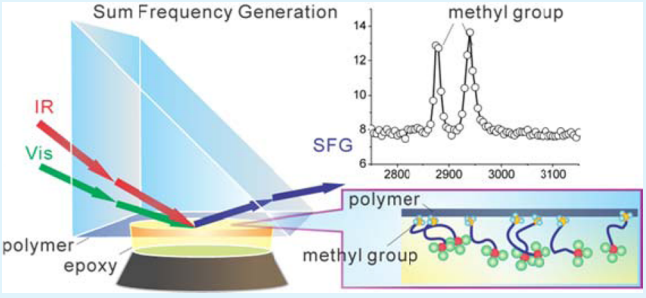

KEYWORDS: *sum frequency generation (SFG), epoxy, polymer, adhesion, interface, silane*

1. INTRODUCTION

The microelectronic industry has advanced rapidly in the last several decades, especially with the invention of and continuous improvements on integrated circuits (IC). The use of flip-chip technology is crucial for the fast development of IC.[1,2] In flip-chip packing, the active side of IC is facing down and connected to the substrate by solder joints. In the early days of flip-chip technology, when IC chips were connected to ceramic substrates, thermal expansion mismatch was not a significant problem because of the small difference in thermal expansion coefficients (TEC) of substrate and die. Later when organic substrates such as polyimide (PI) and poly(ethylene terephthalate) (PET) were used as substrates, significant thermal stress was generated because of the TEC mismatch between the organic substrate and the silicon die.[3] This stress may lead to interfacial fatigue and delamination, causing failure of the device. Therefore, underfill materials were introduced to improve fatigue endurance.[4] In flip-chip technology, underfill resin is used to connect the IC to the substrate through solder joints. Underfill resin is usually dispensed after soldering a chip directly onto the printed circuit board (PCB).[4] After the underfilling, the assembly is heated to cure the underfill resin. The underfill provides both thermo-mechanical and environmental protection of the flip-chip assembly, and makes it stiffer. Therefore, the success of flip-chip technology highly relies on the performance of the underfill materials. Underfill materials are required to possess beneficial characteristics such as good adhesion, high glass transition temperature, and good modulus. Bisphenol-type epoxy resins are most widely used underfill materials,[5] whereas silane molecules are often used in the formulations as adhesion promoters.[6,7]

The delamination between die and underfill or between substrate and underfill may lead to cracking of the interconnection, or moisture diffusion through the delaminated area, resulting in the failure of the device.[8,9] Therefore, underfill adhesion is important for the reliability of the flip-chip assembly, which has been extensively studied. However, almost all the experimental studies up to date focused on macroscopic understanding and have not examined molecular structures of the buried interfaces involving underfill materials in situ. Similarly, most simulations only lead to macroscopic understanding of these interfaces.

Adhesion is a complex and multidisciplinary subject.[7,10−13] In addition to the bulk contributions from the viscoelastic properties of the adhesive, which will be maintained more or less constant in our studies, there exist a number of mechanisms that may contribute to adhesion including interfacial segregation and alignment, interfacial hydrogen and

Received: May 14, 2012
Accepted: June 18, 2012
Published: June 18, 2012

chemical bonding, interfacial diffusion, electrostatic attraction, and mechanical interlocking.[14] As the added silanes in this study have a relatively small impact on the bulk properties at the concentrations used (~1.5%), it is reasonable to expect that adhesion promotion is primarily through interface modification. For interfaces with strong adhesion, it is likely that some strong interactions are operative, perhaps in concert with interdiffusion of certain species.

Adhesion mechanisms largely depend on the molecular interfacial structures and molecular interfacial interactions. Unfortunately, it is very challenging to investigate molecular structures of interfaces due to the lack of appropriate analytical techniques. It is also difficult to investigate buried interfaces in situ. The traditional way to examine a buried interface is to break the interface and examine the two resulting surfaces to extrapolate the molecular structure at the originally buried interface. But such a process may destroy the original interfacial structure, especially for the interfaces with good adhesion. Therefore, a technique which can study buried interfaces in situ at the molecular level is needed.

In recent years, sum frequency generation (SFG) vibrational spectroscopy has been applied to study surfaces and buried interfaces at the molecular level in situ.[15−27] SFG is a nonlinear optical technique which allows probing any surfaces and interfaces that are accessible to laser light. SFG can be used to study interfacial chemical structures and interfacial molecular interactions, such as coverage, orientation, and orientation distribution of interfacial functional groups, interfacial hydrogen bonding formation, interfacial diffusion, etc.[28−33] SFG has also been used to study buried interfaces involving polymers.[32−43] In our lab, SFG has been extensively applied to examine model epoxies for underfill materials and to monitor the epoxy surface/interfacial structural changes after moisture exposure.[38]

In this study, SFG was applied to investigate buried interfaces between epoxy (or epoxy-silane mixture) materials used in packaging and polymers. We specifically probed buried interfaces between a model epoxy, bisphenol A digylcidyl ether (BADGE), and poly(ethylene terephthalate) (PET) before and after curing. Small amounts (1.5 wt %) of four different silanes were added to BADGE to modify the interfacial structures and properties. The effects of the incorporated silanes on buried interfacial structures were observed. In addition, SFG was applied to study the interfaces between two commercial epoxies and two polymers, PET and polystyrene (PS). Adhesion testing experiments were performed to measure the adhesion strengths between epoxies and polymers. The adhesion measurement data can be interpreted by the molecular structures of the buried interfaces deduced from the SFG results. This research is a fundamental step forward to understand the structure−function relationship at interfaces for packaging materials in microelectronic devices. The continuous success in such studies will ultimately lead to the design and development of underfills with improved performances.

2. MATERIALS AND METHODS

2.1. Materials. Fused silica substrates (right angle prisms) were obtained from Altos Photonics, Inc. and used as solid supports for depositing polymer films. Silica prisms were cleaned overnight in a concentrated sulfuric acid bath saturated with potassium dichromate at 60 °C. They were then rinsed using deionized water and dried with nitrogen gas before the polymer film deposition. Aliphatic chain deuterated PET (d_4-PET) was purchased from Polymer Science Inc. The d_4-PET films were prepared by spin coating the 2 wt % d_4-PET solution in 2-chlorophenol (Sigma Aldrich, >99%) on the silica prisms at 2500 rpm. The deuterated polystyrene (d_8-PS) was also obtained from Polymer Science Inc. and the d_8-PS films were prepared using the same method as the d_4-PET films. The solvent used to dissolve d_8-PS is chloroform (Sigma Aldrich >99.8%).

Epoxy curing process is a chemical reaction in which the epoxide groups react with functional groups in the curing agent (hardener) to form a cross-linking network. Amines are the most commonly used curing agents for epoxy curing. In this study, bisphenol A digylcidyl ether (BADGE) was purchased from Sigma-Aldrich. The BADGE samples were cured with diethylenetriamine (DETA) (from Sigma-Aldrich) as curing agent (hardener). Four different silanes: (3-glycidoxypropyl) trimethoxysilane (γ-GPS), (3-Aminopropyl)-trimethoxysilane (ATMS), Octadecyltrimethoxysilane (OTMS(18C)), and Octyltrimethoxysilane (OTMS(8C)) were purchased from Sigma-Aldrich and 1.5 wt % each silane was added to a BADGE sample in each experiment. BADGE epoxies with or without silane added were mixed with DETA and cured in an oven at 50 °C for 4 h. Commercial epoxy resins 3302 (CE3302, transparent and colorless) and 3006 (CE3006, black) were obtained from Epoxies Etc. The main component of both commercial epoxy bases is bisphenol A-(epichlorhydrin) epoxy resin, producing BADGE in the curing process. Small amounts of bis(1,2,2,6,6-pentamethyl-4 piperidinyl)-sebacate and 4-nonylphenol are present in CE3302. The curing agent (hardener) for CE3302 is polyoxypropylenediamine mixed with small amount of 4-nonylphenol. The mixing ratio for resin and hardener is 2:1 by weight. The curing for CE3302 took 2 h at 52 °C. CE3006 contains carbon black with substantial amount of calcium carbonate, small amount of oxirane, mono[(C12−14-alkyloxy)methyl] and 4-nonylphenol. The hardener for CE3006 includes mainly calcium carbonate, polyaminoamide, small amount of tetraethylenepentamine, and benzyl alcohol. The mixing ratio for resin and hardener is 1:1 by weight. The curing for CE3006 took 1 h at 100 °C. All samples were mixed using a vortex mixer (Vortex-Genie 2T, Scientific Industries Inc.) before curing.

Molecular structures of the major materials discussed above which were used in the experiments are shown in Figure. 1. Other chemicals in the two commercial epoxies are listed in the Supporting Information.

2.2. SFG Experiment. SFG is a second-order nonlinear optical process which probes the second order nonlinear susceptibility of the material. The selection rules provide SFG submonolayer surface and interface sensitivity.[26,44,45] This makes SFG a powerful technique for interfacial studies. In a typical SFG system, the visible and mid-infrared

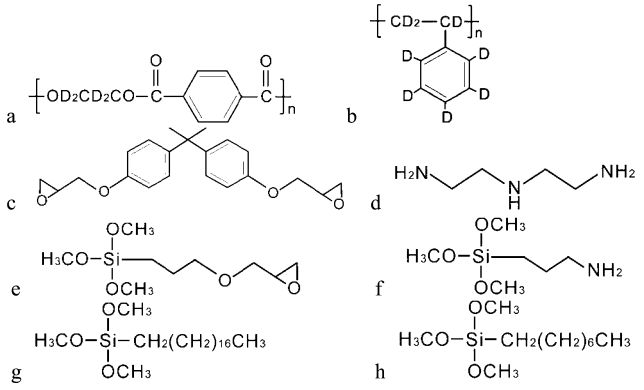

Figure 1. Chemicals used in the experiment: (a) poly(ethylene terephthalate) with aliphatic chain deuterated (d_4-PET), (b) deuterated polystyrene (d_8-PS), (c) bisphenol A digylcidyl ether (BADGE), (d) diethylenetriamine (DETA), (e) (3-glycidoxypropyl) trimethoxysilane (γ-GPS), (f) (3-Aminopropyl)trimethoxysilane (ATMS), (g) octadecyltrimethoxysilane (OTMS(18C)), (h) octyl-trimethoxysilane (OTMS(8C)).

(IR) input beams overlap at the interface (e.g., the polymer/epoxy or polymer/epoxy silane mixture interface) spatially and temporally. In our SFG experiments, both input beams were 20 Hz and contained 20 ps pulses. In this research, the pulse energies were about 30 μJ and 100 μJ for the visible and IR beams, respectively. The SFG signal was generated at the sample interface and collected by a monochromator along with a photomultiplier tube (PMT). The monochromator can be tuned automatically while scanning the IR beam frequency. It took about 2 min to collect an SFG spectrum as displayed below. All SFG spectra in this experiment were collected using the ssp (s-polarized sum frequency output, s-polarized visible input, and p-polarized IR input) polarization combination. SFG spectra were collected from the buried interface between the polymer and epoxy (with or without the addition of silane) before and after curing (Figure 2). Because the aliphatic group deuterated PET and deuterated PS were used in this study, no aliphatic C−H signals would be generated from the buried polymer/substrate interface. The use of prism substrates and the adoption of the experimental geometry shown in Figure 2 greatly enhanced SFG signals compared to the use of the previous experimental geometry utilizing window substrates.[37,39,46]

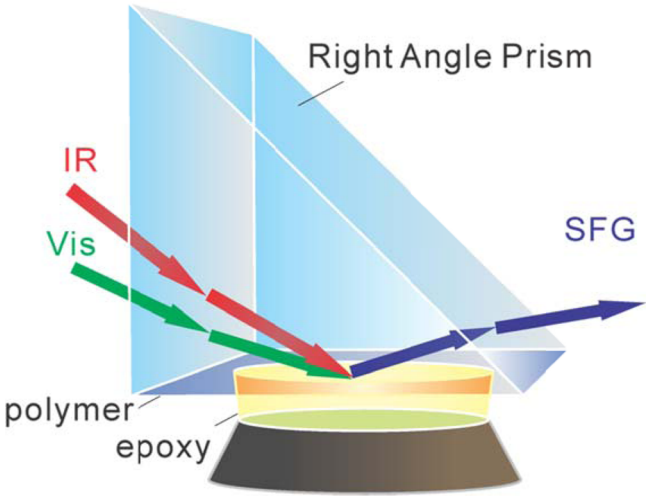

Figure 2. SFG experimental geometry used to study buried polymer/epoxy interfaces. The prism is made of fused silica.

2.3. Adhesion Test. To correlate the molecular level structures at the polymer/epoxy and polymer/epoxy silane mixture interfaces observed by SFG to the physical adhesion strength, we carried out adhesion tests based on the ASTM D3163 Standard with some modifications. The adhesion testing experimental geometry is shown in Figure 3. We cut PET (Ertalyte) or PS (from Small Parts Inc.) sheets into small pieces of the same size. The surfaces of PET and PS sheets (surface area: 24 × 10 mm^2) were sanded and cleaned using deionized water and methonal before use. Two PET (or PS) test pieces were attached by the epoxy or different epoxy-silane mixtures and cured in oven. The adhesive thickness was measured ~0.3 mm. The bonded test pieces were pulled apart at the room temperature with a speed of 1.3 mm/min while the shear strength was measured (using the Instron 5544 mechanical testing instrument). The shear strength is a function of the stretching length, both of which were monitored. When the two sheets were completely separated, a large drop in the adhesion strength occurred. We compared the maximum adhesion strength (measured just before the separation of the two polymer sheets) for various samples. In this research, all the adhesion failures observed are adhesive failures, not cohesive failures. Therefore, the adhesion data we presented here are related to interfacial properties. As we discussed above, because the added silanes in this study have a relatively small impact on the bulk properties at the concentration used (~1.5%), it is reasonable to expect that the adhesion promotion is primarily realized through the changes at the interfaces.

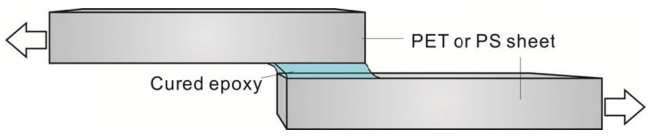

Figure 3. Adhesion test geometry for the 180 degree shear test.

3. RESULTS AND DISCUSSION

3.1. Interfaces between d_4-PET and BADGE. We first collected SFG spectrum from the BADGE epoxy/d_4-PET interface without the addition of the curing agent DETA (Figure 4). Two peaks at 2870 cm^{-1} and 2930 cm^{-1} were detected in the spectrum which can be assigned to the methyl group symmetric C−H stretching mode and Fermi resonance in BADGE. This indicates that the BADGE methyl groups were ordered at this interface. A weak and broad peak at around 3000 cm^{-1} was also observed, which is contributed from the BADGE epoxy ring. Another weak spectral feature detected at around 3100 cm^{-1} should be contributed by the aromatic C−H stretching modes from the phenyl group in d_4-PET. This shows that the phenyl ring in d_4-PET also presents with some order at the BADGE/d_4-PET interface.

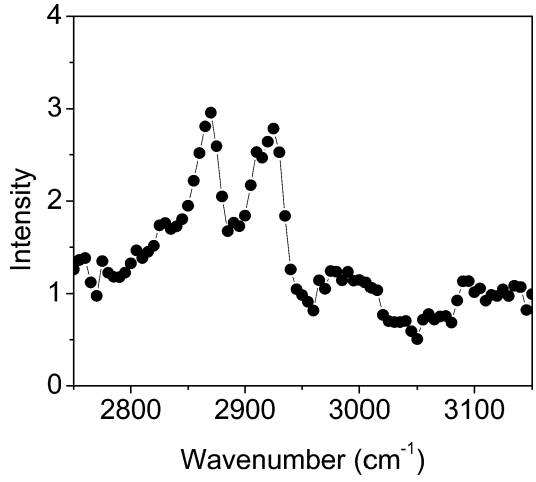

Figure 4. SFG spectrum collected from the BADGE (without the curing agent DETA)/d_4-PET interface.

We then collected SFG spectra of BADGE and different BADGE silane mixtures in contact with d_4-PET before and after curing with the addition of the curing agent DETA. We mixed BADGE with the curing agent DETA to form a homogeneous mixture, and contacted the mixture with spin coated d_4-PET thin film. SFG spectra were collected from the BADGE/d_4-PET interface (Figure 5a). Before curing, a weak and broad peak at ~2950 cm^{-1} could be resolved, may due to the Fermi resonance of the BADGE methyl group, indicating that BADGE methyl groups may adopt some order at the interface. It is interesting to observe that this spectrum is markedly different from that shown in Figure 4; the overall SFG C−H stretching signal decreased greatly compared to the case before the addition of the curing agent. This demonstrates that the addition of the curing agent changed the interfacial structure substantially. Some of the curing agent molecules can segregate

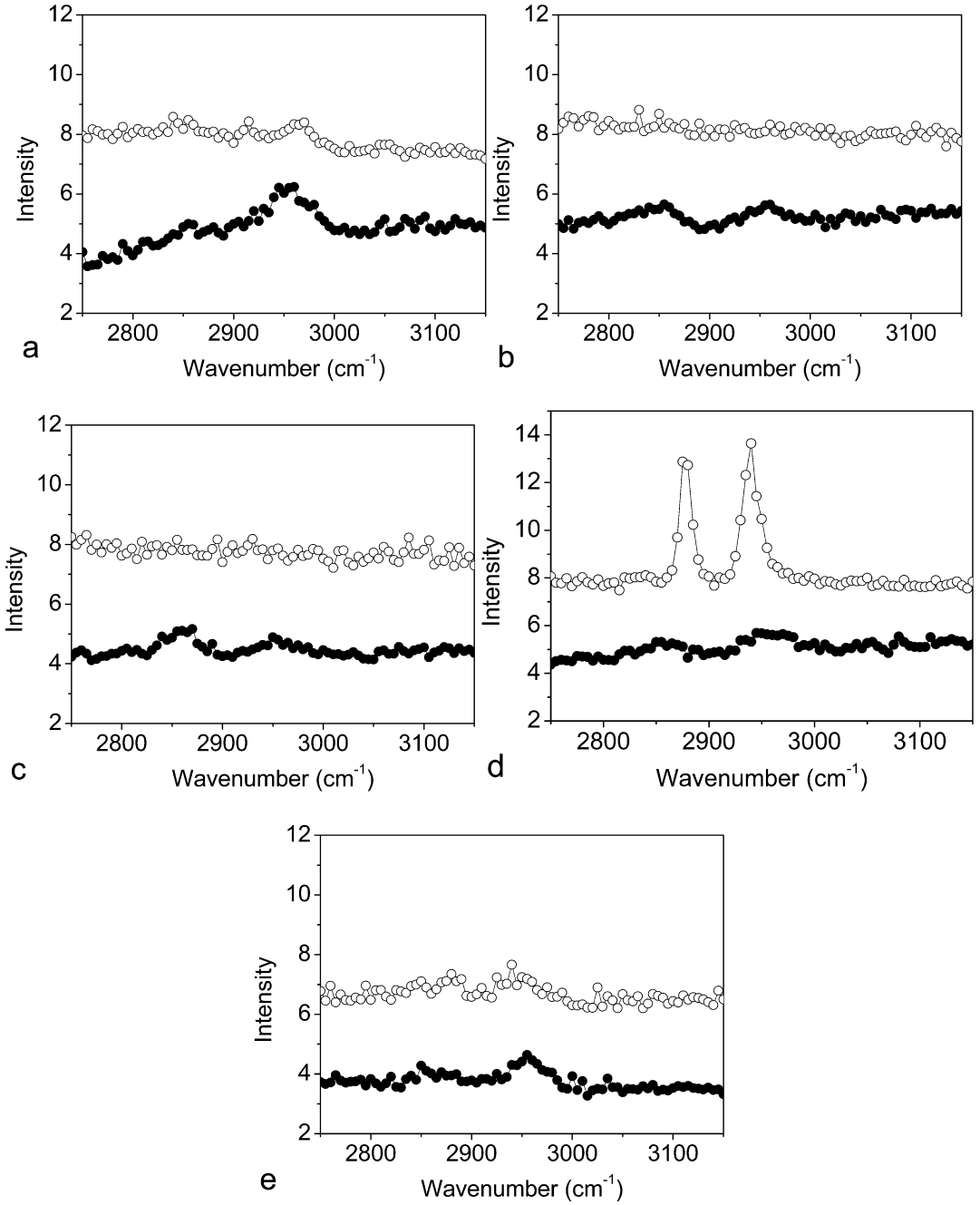

Figure 5. SFG spectra collected from (a) BADGE/d_4-PET interface, (b) BADGE+ γ-GPS/d_4-PET interface, (c) BADGE+ ATMS/d_4-PET interface, (d) BADGE+ OTMS(18C)/d_4-PET interface, (e) BADGE+ OTMS(8C)/d_4-PET interface. Closed dots: spectra collected before curing. Open dots: spectra collected after curing. The spectral range is from 2750 to 3150 cm^{-1}.

to the interface to disorder the interfacial BADGE molecules. Because the curing agent itself has a symmetric structure, it generates no SFG C−H stretching signals. After curing, almost no signal can be detected, indicating that the curing process disordered the BADGE methyl groups at the interface.

After we studied the BADGE/d_4-PET interface before and after curing, we added small amounts (1.5 wt %) of four different silanes to mix with BADGE and DETA homogeneously before curing. We studied the mixture using SFG in C−H spectral range (2750−3150 cm^{-1}). Similar spectral features were observed from the interfaces before curing when different silanes including γ-GPS, ATMS, OTMS (18C) and OTMS (8C) were added to the systems. The SFG signals were all weak and showed two weak peaks at ∼2850 and ∼2950 cm^{-1} in C−H range, due to the methylene symmetric C−H stretching and methyl Fermi resonance. This shows that the addition of small amount (1.5 wt %) of various silanes does not substantially influence the interfacial structure before curing.

The samples were then cured at 50 °C for 4 h. SFG spectra collected from the above interfaces in C−H range after curing are substantially different. No SFG signal in the C−H stretching frequency region was detected from the interfaces between d_4-PET and BADGE mixed with γ-GPS and ATMS respectively. We believe that γ-GPS and ATMS can segregate to the interface. The disappearance of the SFG signals from these two interfaces may be due to the disordering of the interfacial

silanes and/or the interfacial diffusion of silanes across the interface and the interface was not distinct anymore (Figure 5b, c). It has been shown extensively that interfacial diffusion can lead to the enhancement of adhesion.[47−50] Differently, the SFG spectrum collected from the BADGE (with 1.5 wt % OTMS(18C))/d_4-PET interface after curing exhibits two strong peaks at 2880 and 2940 cm^{-1} respectively (Figure 5d). These two peaks are assigned to the methyl end group C−H symmetric stretching and Fermi resonance in OTMS. This indicates that after curing, OTMS end groups became ordered at the BADGE/d_4-PET interface. The largest differences among γ-GPS, ATMS, and OTMS (18C) are that they have different end groups, as epoxy, amino, and methyl groups respectively. Therefore the silane end groups greatly impact the interfacial structures between BADGE (mixed with 1.5 wt % silane) and d_4-PET.

We also collected SFG spectrum from the interface between d_4-PET and BADGE mixed with 1.5 wt % OTMS(8C) after curing. The silane OTMS(8C) has a shorter chain than OTMS(18C). SFG spectrum collected from this interface is markedly different from the case when OTMS(18C) was added (Figure 5(e)). Only very weak signal was observed in the spectrum. This means at the interface of epoxy and PET, OTMS(8C) does not have strong order. This also demonstrates that the silane chain length impacts the interfacial structure. If the disappearance of signal is caused by the silane interfacial diffusion, then perhaps the shorter silane molecules can diffuse into the polymer matrix easier.

All four types of silanes studied here are methoxy silanes which have methoxy head groups. The C−H symmetric stretching signal of a methoxy group is centered at 2845 cm^{-1}, which was not observed in the experiment using SFG. This indicates that the methoxy head groups are not ordered at the interfaces. Moreover, all four types of silanes have backbones, which are composed of methylene groups. The C−H symmetric and asymmetric stretching signals of methylene groups are at 2850 and 2920 cm^{-1} respectively, which were not observed either after curing.

For end group effect, both OTMS molecules (with different chain lengths) have methyl end groups, but only OTMS (18C) shows significant methyl C−H signal at the interface after curing. This means that OTMS (18C) methyl end group tends to adopt some order at the interface after curing, whereas OTMS (8C) molecules at the interface tend to have disordered methyl end groups. The γ-GPS' end group is an epoxy ring, which should generate SFG signal at 3000 cm^{-1} when ordered. We did not observe any SFG signal at the interface for the epoxy ring, thus we believe that the end group in γ-GPS is disordered at the interface. For ATMS, the end group has N−H bonds, which should contribute a peak at 3300 cm^{-1} when adopting some order. We collected SFG spectra from the BADGE/d_4-PET interfaces before and after curing in the N−H stretching frequency range (3100−3600 cm^{-1}). The results are shown in Figure 6. Before curing, N−H stretching signal at 3300 cm^{-1} can be observed, contributed by the ATMS -NH_2 end group and/or amines in DETA. After curing, N−H stretching signal disappeared. This indicates that ATMS −NH_2 end groups may adopt some order at BADGE/d_4-PET interface before curing, but disorder or disappear at the interface after curing. End group -NH_2 in ATMS tend to form hydrogen bonding with PET,[32] which may lead to the order of N−H groups at the interface. Or, more likely, amine end groups of ATMS reacted with epoxy similar to amines in DETA. The

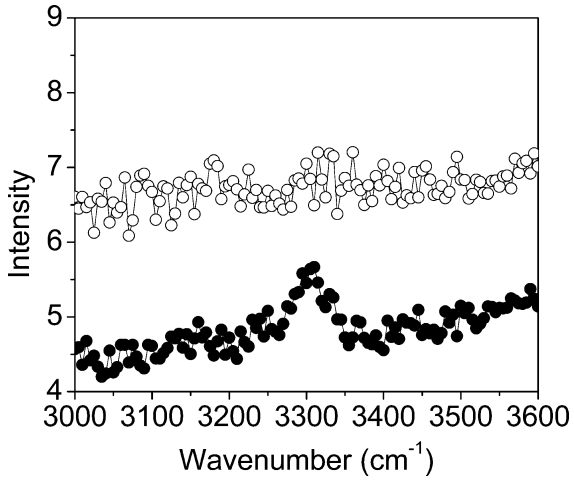

Figure 6. SFG spectra collected at BADGE+ATMS/d_4-PET interface. Bottom spectrum: before curing; Top spectrum: after curing. The spectral range is from 3000 to 3600 cm^{-1}.

curing process may break hydrogen bonding and disorders ATMS end groups at the interface. Therefore for all the four types of silanes studied here, only methyl end groups in OTMS(18C) are strongly ordered at the interface after curing process.

The adhesion testing experiments were carried out after curing the various interfaces (Figure 7). All these samples are

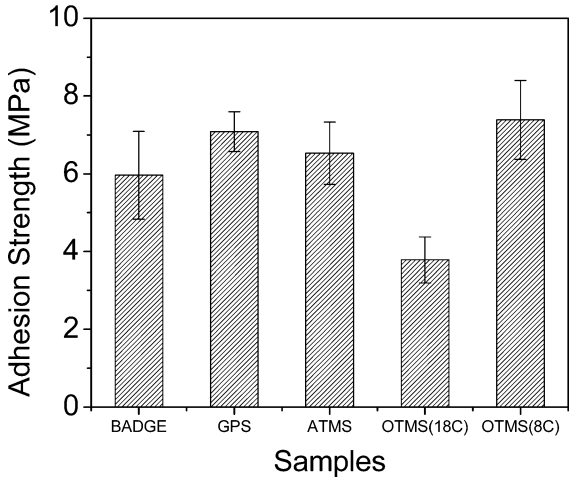

Figure 7. Adhesion testing results of model epoxy BADGE and BADGE silane mixtures to PET after curing. Adhesion strength = maximum adhesion force/contact area.

only slightly different in bulk content: Four samples have only 1.5 wt % of different silanes in the system, whereas the fifth sample does not contain any silane. The adhesion testing results indicated clearly that the small amounts of silane incorporated into the epoxy mixtures can alter the adhesion properties. The addition of γ-GPS, ATMS, and OTMS(8C) to BADGE slightly increased the adhesion to d_4-PET while the addition of OTMS(18C) strongly decreased the adhesion. The adhesion data can be well correlated to the SFG measurements. Only the SFG spectrum collected from the interface after the addition of OTMS(18C) shows large methyl signal, indicating silane methyl end group order at the interface, which leads to weak adhesion. Almost no SFG signal could be detected from

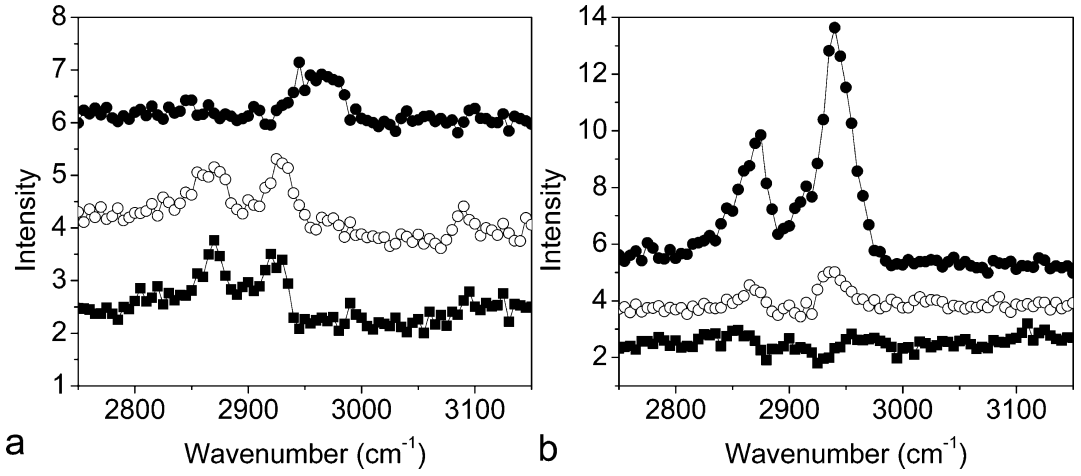

Figure 8. SFG spectra collected from (a) the CE3302/d_4-PET interface; (b) the CE3302/d_8-PS interface. From the top to the bottom: SFG spectra from interfaces of the cured sample, the uncured sample, and the epoxy base without hardener.

the cured interfaces after the additions of γ-GPS, ATMS, and OTMS(8C) into BADGE, indicating that these interfaces have disordered molecular structures. The interfacial disordered structure is caused by the randomization of the molecules at the interface, or interfacial diffusion, or chemical reaction, all of which can enable more entanglements of various molecular chains, resulting in stronger adhesion at the interface. We believe that the methyl ordering at the interface leads to weak adhesion because methyl groups cannot form stronger interactions than van der Waals interactions.

3.2. Interfaces between Polymer and Commercial Epoxies. We extended our research from model epoxy BADGE to commercial epoxies. We investigated two commercial underfill epoxies CE3302 and CE3006 which have the same BADGE main component. We first collected SFG spectra from the d_4-PET/CE3302 interfaces (Figure 8a). Without the curing agent, the detected SFG spectrum shows similar features compared to that detected from the BADGE/d_4-PET interface. Two peaks at 2870 and 2930 cm^{-1} were detected, which are contributed by the methyl groups in the epoxy. After adding the curing agent to CE3302, the detected SFG spectrum from this interface did not change substantially, which is different from the model epoxy BADGE case reported above. Perhaps here the ordered methyl groups at the interface are those from other components in CE3302 such as bis(1,2,2,6,6-pentamethyl-4 piperidinyl)sebacate and 4-nonylphenol, which do not exist in the model BADGE epoxy. After curing, the strong methyl group symmetric C−H stretch in the SFG spectrum disappeared, while only a weak methyl asymmetric C−H stretching signal was detected. This is similar to the model BADGE case reported above.

We also collected SFG spectra from the d_8-PS/CE3302 interfaces. As shown in Figure 8b, pure CE3302 base does not exhibit methyl group ordering at the interface with d_8-PS. This indicates that CE3302 can have different interfacial molecular structures while in contact with different polymers, due to different molecular interactions. After the addition of the curing agent, methyl groups started to order at the d_8-PS/CE3302 interface, similar to the d_4-PET case. After curing, different from the d_4-PET case, strong methyl group signals were detected at 2875 and 2935 cm^{-1}. This means that the methyl groups are very ordered at the interface with d_8-PS. According to the SFG and adhesion studies on the model epoxy BADGE reported above, we know that the disappearance of the SFG signals usually leads to strong adhesion, and methyl group interfacial ordering usually leads to weak adhesion. Therefore, we can predict that the cured PET/CE3302 interface should have stronger adhesion, while the cured PS/CE3302 interface should have weaker adhesion. This was proved by the data acquired from the adhesion testing experiments. The adhesion testing results are shown in Figure 9. Clearly, CE3302 has much stronger adhesion to PET compared to PS.

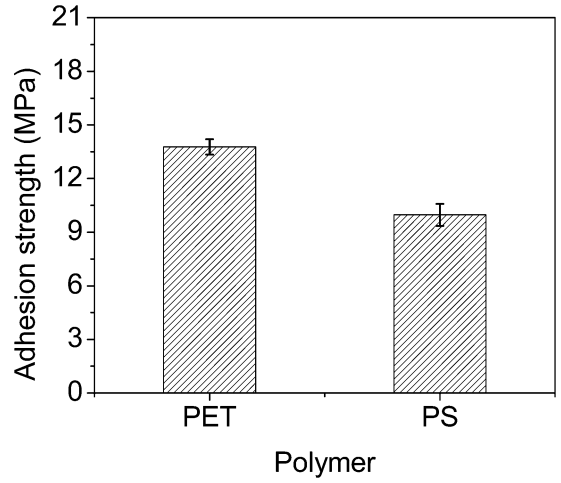

Figure 9. Adhesion testing results of commercial epoxy 3302 to PET and PS.

In addition to CE3302, we studied another commercial epoxy CE3006, which is a black epoxy due to its carbon black ingredient. We first collected the SFG spectrum from the d_4-PET/CE3006 interface before the addition of the curing agent. Broad peaks at 2930 and 2960 cm^{-1} were detected (Figure 10a), which are assigned to the methyl groups in epoxy. This spectrum is different from those collected from the d_4-PET/pure BADGE interface and the d_4-PET/CE3302 (without hardner) interface cases. This means that the calcium carbonate ingredient in the sample could affect the interfacial structure. After adding the curing agent, in addition to the methyl signals, SFG signal from methylene groups could also be detected at 2850 cm^{-1}. However, after curing, no SFG signal could be

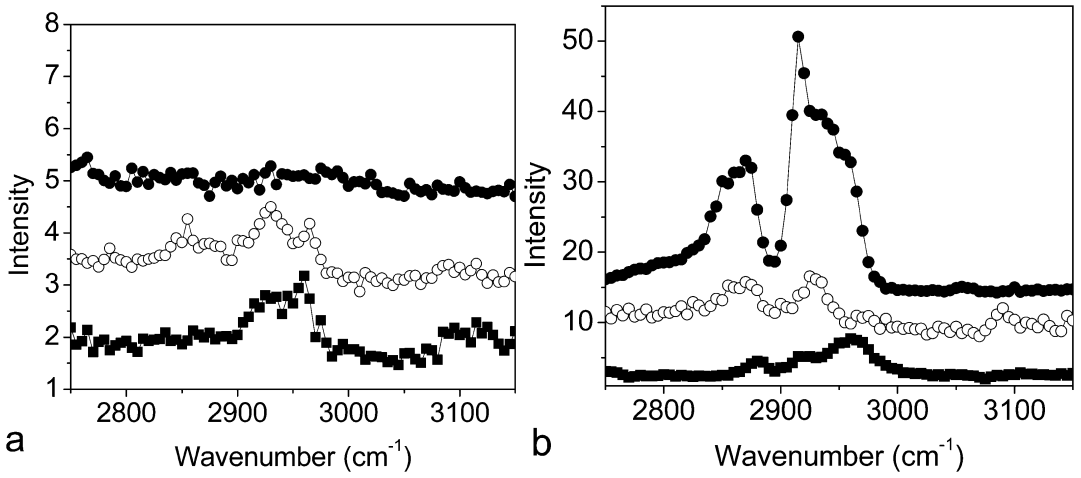

Figure 10. SFG spectra collected from (a) the CE3006/d_4-PET interface; (b) the CE3006/d_8-PS. From the top to the bottom: SFG spectra from interfaces of the cured sample, the uncured sample, and the epoxy base without hardener. For spectrum in the middle of b, it is multiplied by a factor of 5.

detected from the interface, indicating the interfacial diffusion and/or interfacial disordering (Figure 10a). We then studied the d_8-PS/CE3006 interfaces. Before the addition of the curing agent, methyl groups are ordered at the interface, evidenced by the observed methyl symmetric and asymmetric stretching signals at 2880 and 2960 cm^{-1}, respectively (Figure 10b). Another peak at 2920 cm^{-1} could also be observed, indicating that methylene groups also adopt some order at the interface. After the addition of the hardener or curing agent, methyl groups are still ordered at the interface. After curing, much stronger SFG signals were detected at 2850, 2880, 2920, 2940, and 2960 cm^{-1}, showing that both methyl and methylene groups are highly ordered at the interface (Figure 10b). From SFG studies, we can again predict that the PET/CE3006 interface has stronger adhesion while the PS/CE3006 interface has weaker adhesion. The adhesion testing results again proved this prediction, as shown in Figure 11.

4. SUMMARY

In this study, we demonstrated that SFG is a powerful technique to investigate molecular structures of buried interfaces in situ between polymers and underfill materials. A model epoxy and two commercial epoxy resins were investigated. In the model epoxy study, small amounts of different silanes (1.5 wt %) were added to the epoxy, which substantially influenced the polymer/epoxy interfacial structures and interfacial adhesion. Both silane end groups and chain length play roles in silane behaviors at the buried interfaces. The segregation and disordering of silanes with epoxy end groups, amino end groups, and short chains at the interface, along with the interfacial disordering of the epoxy compounds, lead to strong adhesion. The long chain silane with methyl end groups exhibits methyl ordering at the interface, reducing adhesion. This conclusion was supported by SFG studies on two commercial epoxy resins. SFG studies indicated that the molecular disorder may occur from both commercial resins while in contact with PET after curing, and strong adhesion was measured. Methyl group ordering at the interface was observed for these two commercial epoxies while in contact with PS after curing, and weak adhesion was measured.

We believe this is the first report to investigate correlations between molecular structures of interfaces and adhesion involving commercial underfill materials. We have demonstrated that SFG is a powerful tool to elucidate molecular mechanisms for adhesion at buried interfaces. In the future, adhesion promoting systems with different deuterated components need to be used. This will further differentiate SFG signals in the C−H spectral region and allow us to elucidate more detailed molecular structures of buried interfaces and more detailed structure−adhesion correlations.

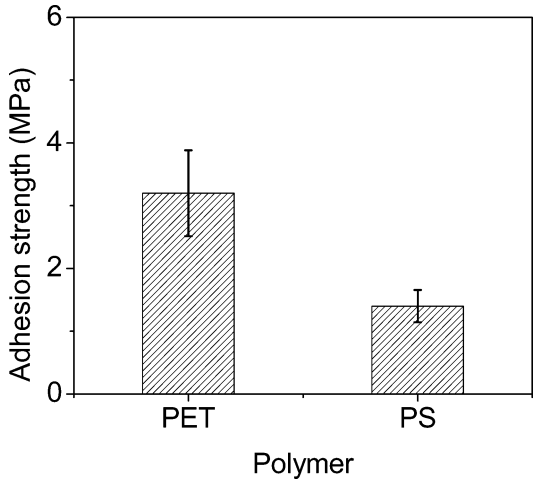

Figure 11. Adhesion testing results of CE3006 to PET and PS.

■ ASSOCIATED CONTENT

Supporting Information

Chemicals in the two commercial epoxies. This material is available free of charge via the Internet at http://pubs.acs.org/.

■ AUTHOR INFORMATION

Corresponding Author

*Fax: +1 734 647 4865. E-mail: zhanc@umich.edu.

Notes

The authors declare no competing financial interest.

■ ACKNOWLEDGMENTS

This work is supported by the semiconductor research corporation (SRC P10419 and P13696).

■ REFERENCES

(1) Tong, H. M. *Mater. Chem. Phys.* **1995**, *40*, 147−161.
(2) Wong, C. *Mater. Chem. Phys.* **1995**, *42*, 25−30.
(3) Sham, M. L.; Kim, J. K. *J. Electron. Packag.* **2005**, *127*, 47−51.
(4) Kornain, Z.; Jalar, A.; Rasid, R.; Abdullah, S. *J. Electron. Packag.* **2010**, *132*, 041012.
(5) Luo, S. J.; Yamashita, T.; Wong, C. P. *J. Electron. Manuf.* **2000**, *10*, 191−200.
(6) Yung, K. C.; Liem, H. *J. Appl. Polym. Sci.* **2007**, *106*, 3587−3591.
(7) Yacobi, B. G.; Martin, S.; Davis, K.; Hudson, A.; Hubert, M. *J. Appl. Phys.* **2002**, *91*, 6227−6262.
(8) Hegde, S.; Pucha, R. V.; Sitaraman, S. K. *J. Mater. Sci−Mater. Electron.* **2004**, *15*, 287−296.
(9) Zhang, Y. L.; Shi, D. X. Q.; Zhou, W. *Microelectron. Reliab.* **2006**, *46*, 409−420.
(10) Newby, B. M. Z.; Chaudhury, M. K.; Brown, H. R. *Science* **1995**, *269*, 1407−1409.
(11) Sathyanarayana, M. N.; Yaseen, M. *Prog. Org. Coat.* **1995**, *26*, 275−313.
(12) Pocius, A. V. *Adhesion and Adhesives Technology: An Introduction*; Hanser Gardner: Cincinnati, OH, 1997.
(13) Harding, P. H.; Berg, J. C. *J. Appl. Polym. Sci.* **1998**, *67*, 1025−1033.
(14) Kinloch, A. J. *Adhesion and Adhesives: Science and Technology*; Chapman & Hall: London, 1987.
(15) Shen, Y. *Nature* **1989**, *337*, 519−525.
(16) Chen, Z.; Shen, Y.; Somorjai, G. A. *Annu. Rev. Phys. Chem.* **2002**, *53*, 437−465.
(17) Kataoka, S.; Cremer, P. S. *J. Am. Chem. Soc.* **2006**, *128*, 5516−5522.
(18) Baldelli, S. *Acc. Chem. Res.* **2008**, *41*, 421−431.
(19) Ye, S.; Morita, S.; Li, G. F.; Noda, H.; Tanaka, M.; Uosaki, K.; Osawa, M. *Macromolecules* **2003**, *36*, 5694−5703.
(20) Holinga, G. J.; York, R. L.; Onorato, R. M.; Thompson, C. M.; Webb, N. E.; Yoon, A. P.; Somorjai, G. A. *J. Am. Chem. Soc.* **2011**, *133*, 6243−6253.
(21) Hayes, P. L.; Keeley, A. R.; Geiger, F. M. *J. Phys. Chem. B* **2010**, *114*, 4495−4502.
(22) Perry, A.; Neipert, C.; Space, B.; Moore, P. B. *Chem. Rev.* **2006**, *106*, 1234−1258.
(23) Buck, M.; Himmelhaus, M. *J. Vac. Sci. Technol., A* **2001**, *19*, 2717−2736.
(24) Williams, C. T.; Beattie, D. A. *Surf. Sci.* **2002**, *500*, 545−576.
(25) Chen, P.; Kung, K. Y.; Shen, Y. R.; Somorjai, G. A. *Surf. Sci.* **2001**, *494*, 289−297.
(26) Moad, A. J.; Simpson, G. J. *J. Phys. Chem. B* **2004**, *108*, 3548−3562.
(27) Jayathilake, H. D.; Driscoll, J. A.; Bordenyuk, A. N.; Wu, L. B.; da Rocha, S. R. P.; Verani, C. N.; Benderskii, A. V. *Langmuir* **2009**, *25*, 6880−6886.
(28) Chen, Z. *Polym. Int.* **2007**, *56*, 577−587.
(29) Chen, Z. *Prog. Polym. Sci.* **2010**, *35*, 1376−1402.
(30) Chen, C. Y.; Wang, J.; Even, M. A.; Chen, Z. *Macromolecules* **2002**, *35*, 8093−8097.
(31) Chen, C. Y.; Loch, C. L.; Wang, J.; Chen, Z. *J. Phys. Chem. B* **2003**, *107*, 10440−10445.
(32) Loch, C. L.; Ahn, D.; Chen, C. Y.; Wang, J.; Chen, Z. *Langmuir* **2004**, *20*, 5467−5473.
(33) Chen, C. Y.; Wang, J.; Loch, C. L.; Ahn, D.; Chen, Z. *J. Am. Chem. Soc.* **2004**, *126*, 1174−1179.
(34) Lu, X. L.; Clarke, M. L.; Li, D. W.; Wang, X. P.; Xue, G.; Chen, Z. *J. Phys. Chem. C* **2011**, *115*, 13759−13767.
(35) Lu, X. L.; Shephard, N.; Han, J. L.; Xue, G.; Chen, Z. *Macromolecules* **2008**, *41*, 8770−8777.
(36) Ohe, C.; Kamijo, H.; Arai, M.; Adachi, M.; Miyazawa, H.; Itoh, K.; Seki, T. *J. Phys. Chem. C* **2008**, *112*, 172−181.
(37) Vázquez, A. V.; Boughton, A. P.; Shephard, N. E.; Rhodes, S. M.; Chen, Z. *ACS Appl. Mater. Interfaces* **2009**, *2*, 96−103.
(38) Vázquez, A. V.; Holden, B.; Kristalyn, C.; Fuller, M.; Wilkerson, B.; Chen, Z. *ACS Appl. Mater. Interfaces* **2011**, *3*, 1640−1651.
(39) Vázquez, A. V.; Shephard, N. E.; Steinecker, C. L.; Ahn, D.; Spanninga, S.; Chen, Z. *J. Colloid Interface Sci.* **2009**, *331*, 408−416.
(40) Kweskin, S. J.; Komvopoulos, K.; Somorjai, G. A. *Langmuir* **2005**, *21*, 3647−3652.
(41) Kweskin, S. J.; Komvopoulos, K.; Somorjai, G. A. *Appl. Phys. Lett.* **2006**, *88*, 134105.
(42) Morita, S.; Ye, S.; Li, G. F.; Osawa, M. *Vib. Spectrosc.* **2004**, *35*, 15−19.
(43) Harp, G. P.; Rangwalla, H.; Yeganeh, M. S.; Dhinojwala, A. *J. Am. Chem. Soc.* **2003**, *125*, 11283−11290.
(44) Hirose, C.; Akamatsu, N.; Domen, K. *Appl. Spectrosc.* **1992**, *46*, 1051−1072.
(45) Löbau, J.; Wolfrum, K. *J. Opt. Soc. Am. B* **1997**, *14*, 2505−2512.
(46) Zhang, C.; Shephard, N. E.; Rhodes, S. M.; Chen, Z. *Langmuir* **2012**, *28*, 6052−6059.
(47) Brown, H. R. *Macromolecules* **2001**, *34*, 3720−3724.
(48) Kulasekere, R.; Kaiser, H.; Ankner, J. F.; Russell, T. P.; Brown, H. R.; Hawker, C. J.; Mayes, A. M. *Macromolecules* **1996**, *29*, 5493−5496.
(49) Sikka, M.; Pellegrini, N. N.; Schmitt, E. A.; Winey, K. I. *Macromolecules* **1997**, *30*, 445−455.
(50) Bernard, B.; Brown, H. R.; Hawker, C. J.; Kellock, A. J.; Russell, T. P. *Macromolecules* **1999**, *32*, 6254−6260.